

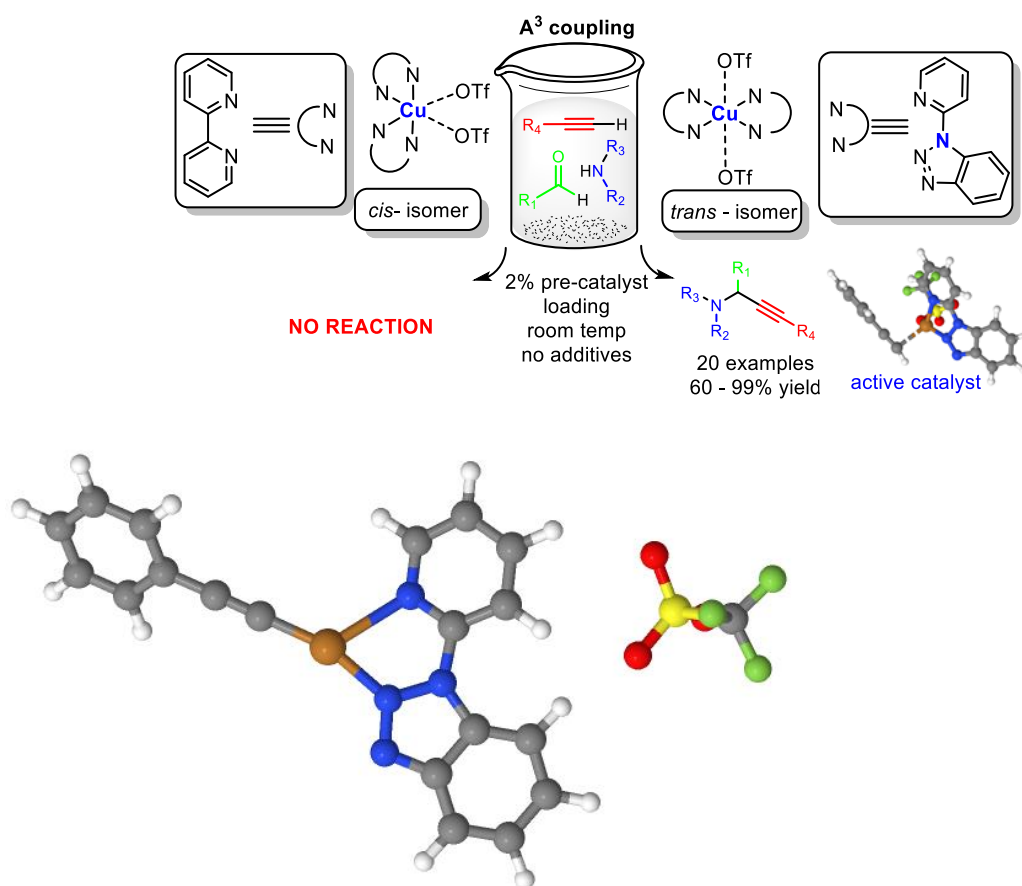
## Structural and electronic control of 1-(2-pyridyl)benzotriazole bidentate ligand in copper chemistry with application to catalysis in the $A^3$ coupling reaction

Stavroula I. Sampani,<sup>a</sup> Victor Zdorichenko,<sup>b</sup> Jack Devonport,<sup>a</sup> Gioia Rossini,<sup>a</sup> Matthew Leech,<sup>c</sup> Kevin Lam,<sup>c</sup> Brian Cox,<sup>a,b</sup> Alaa Abdul-Sada,<sup>a</sup> Alfredo Vargas<sup>a\*</sup> and George E. Kostakis<sup>a\*</sup>

<sup>a</sup>Department of Chemistry, School of Life Sciences, University of Sussex, Brighton BN1 9QJ, UK. E-mail: [Alfredo.Vargas@sussex.ac.uk](mailto:Alfredo.Vargas@sussex.ac.uk) & [G.Kostakis@sussex.ac.uk](mailto:G.Kostakis@sussex.ac.uk)

<sup>b</sup>Photodiversity Ltd c/o Department of Chemistry, School of Life Sciences, University of Sussex, Brighton BN1 9QJ, UK.

<sup>c</sup>School of Science, Department of Pharmaceutical Chemical and Environmental Sciences, University of Greenwich, Central Avenue, Chatham Maritime, ME4 4TB, UK.

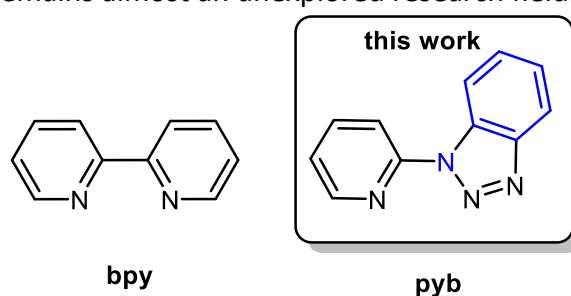


### Abstract

We introduce the hybrid bidentate 1-(2-pyridyl)benzotriazole (pyb) ligand in 3d-transition metal catalysis. Specifically,  $[Cu(II)(pyb)_2(OTf)_2] \cdot 2(CH_3CN)$  (**1**) enables the synthesis of a wide range of propargylamines, via the  $A^3$  coupling reaction, at room temperature, in open-air and absence of additives. The labile character of the bridging N atom of the hybrid ligand is the key parameter that imposes the sole form of the *trans*-isomer and simultaneous ligand rotation, thus orchestrating structural and electronic catalyst control and permitting alkyne binding with concomitant activation of the C–H bond.

Copper is a labile transition metal, plural in oxidation states that promotes a variety of organic transformations either as a metal salt, *in situ* formed or well-characterised complexes.<sup>[4,2]</sup> In its dominant oxidation state(II), the d<sup>9</sup> electronic configuration profound elongated or shorten axial axes, known as Jahn and Teller effect,<sup>[3]</sup> and depending on the coordinating ligands various geometries and stereoisomers, i.e. *cis* – *trans* for Cu(N-N)<sub>2</sub>X<sub>2</sub> where N-N is a bidentate ligand, can be obtained. 2,2-bipyridine (bpy) has been extensively used in coordination chemistry as a bidentate ligand<sup>[4]</sup> and catalysis.<sup>[5]</sup> The catalytic protocols that involve *in situ* blending of bpy, copper salts and substrates achieve high yields and new products;<sup>[6]</sup> however, the role of each component in the catalytic cycle is questioned. Well characterised Cu(II) and bpy based complexes have been used as models for the aerobic oxidation of alcohols<sup>[7]</sup> and other organic transformations.<sup>[8]</sup> In some occasions, well-characterised Cu(II)-bpy complexes surpass the catalytic performance of isostructural compounds built with similar N,N'-bidentate ligands. This differentiation in catalytic efficacy may be a result of electronic and/or steric effects; however, the formation of different stereoisomers cannot be ignored.<sup>[9]</sup>

The importance of developing the coordination chemistry of new bidentate ligands and identifying better catalysts is fundamental. Our groups initiated a combined, experimental and theoretical, project to provide an in-depth description and understanding of the properties that govern the chemistry of the 1-(2-pyridyl)benzotriazole (pyb) ligand (Scheme 1) and the resulting coordination complexes. When compared with bpy, the hybrid pyb ligand, has the following differences: a) additional N atoms that may participate in H-bonding interactions, b) another phenyl group that enforces an electron-rich character of the framework but also permits participation in stacking interactions, and c) the two, pyridine and benzotriazole, units are linked via an N atom, in which its lone electron pair may impose flexibility yielding different coordination behaviour when compared with the rigid C-C based bpy ligand. Steel, in his pioneer work, identified pyb-based compounds to be more electron-deficient when compared with that of bpy,<sup>[10]</sup> however, the applicability of pyb-based complexes in catalysis remains almost an unexplored research field.<sup>[11-14]</sup>



**Scheme 1.** The traditional bidentate ligand 2,2'-bipyridine (bpy) and the bidentate ligand used in this work.

Following a previously described protocol,<sup>[10]</sup> the ligand pyb (Fig S1) can be made in one, high yielding, step from the alkylation reaction of 2-bromopyridine and benzotriazole, while the use of microwaves improves yield and rate (see ESI). The room temperature reaction of Cu(OTf)<sub>2</sub> and pyb in a molar ratio 1 :2, in CH<sub>3</sub>CN under aerobic conditions, yields compound [Cu(pyb)<sub>2</sub>(OTf)<sub>2</sub>]-2(CH<sub>3</sub>CN) (**1**) in 85% yield. Compound **1** is characterised by single-crystal x-ray diffraction, ESI-MS (Fig S2-4), UV-Vis (Fig S5), IR (Fig S6), thermogravimetric (Fig S7) and elemental analysis and cyclic voltammetry (Fig S8). Copper adopts a *trans* geometry and sits in the centre of an octahedron; the equatorial positions are occupied by two pyb ligands, while two OTf<sup>-</sup> anions hold the axial positions. There is a significant difference

between the Cu-N and the Cu-O bonds, which is characteristic of the Jahn-Teller distortion. Bond valence calculations are in line for a Cu(II) oxidation state. Solution studies (ESI-MS) identify the stability of this compound exhibiting only two peaks at 604.0338 m/z and 407.9566 m/z which correspond to the  $[\text{Cu(II)}\text{L}_2(\text{OTf})]^+$  and  $[\text{Cu(II)}\text{L}(\text{OTf})]^+$  species, respectively (Fig S2). The UV-Vis in a solution of dichloromethane shows a very broad (550-850nm) peak with the maximum at 685nm, characteristic of a Cu(II) with Jahn Teller distortion(Fig S5). Besides, the cyclic voltammogram of **1** shows a reversible one-electron curve (Fig S8).

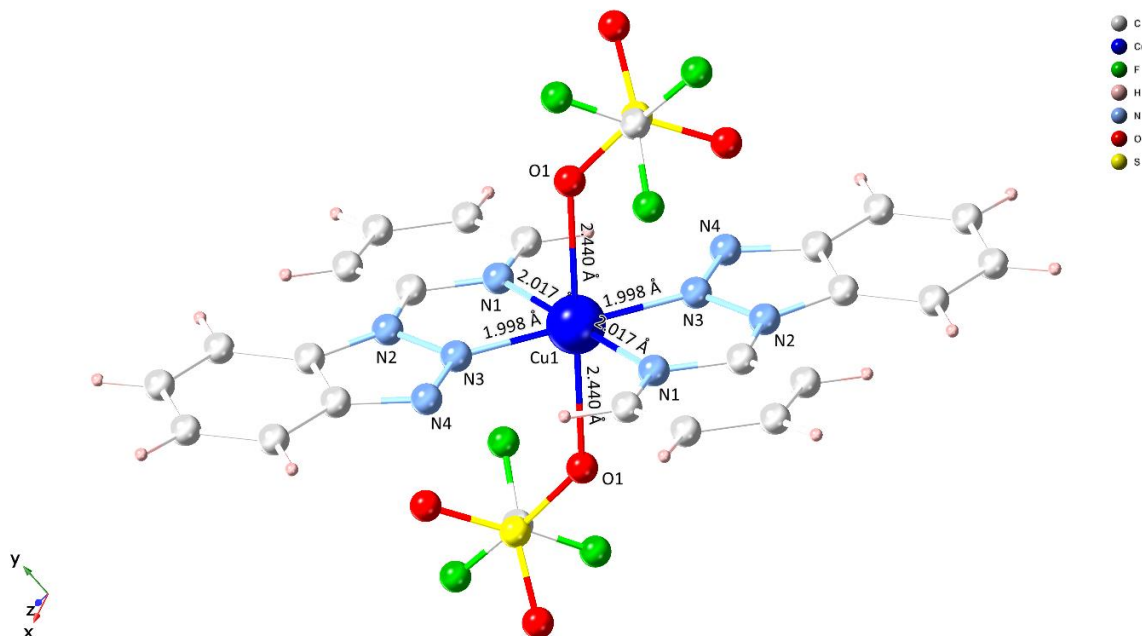


**Figure 1.** The X-ray structure of compound **1**. The  $\text{CH}_3\text{CN}$  lattice molecules are omitted for clarity.

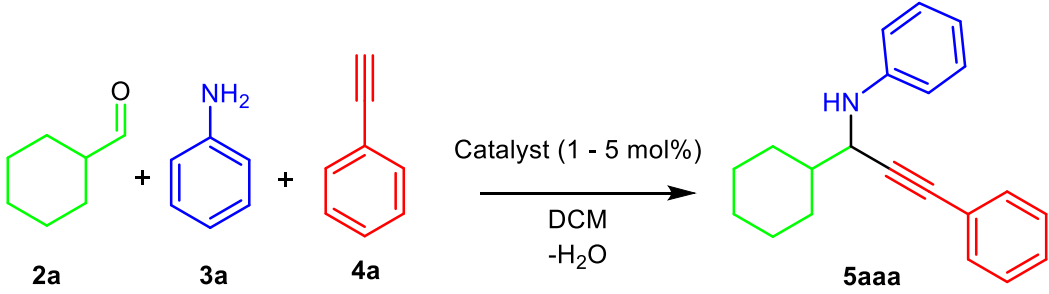
With the catalyst in hand, the next step was to identify a challenging reaction. The  $\text{A}^3$  coupling is a very well known, atom efficient, reaction that yields propargylamines<sup>[15–17]</sup> with one molecule of water as a side product. Methodologies that involve Cu(II) sources have been reported,<sup>[18–22]</sup> however, the emphasis, in these studies, is given in the final product and achieving excellent yields, irrespectively of the extreme reaction conditions, i.e. elevated temperatures, prolonged time, high catalyst loadings; therefore mechanistic details are built based on the experimental findings. On the other hand, Knochel's pioneer work determines the activation of the acetylide on the coordination sphere of the Cu(I) centre and subsequently coupling with the corresponding imine.<sup>[23]</sup> Besides, copper reduction may occur in the presence of alkynes, and this process depends on temperature and concentration.<sup>[24]</sup>

Taking into account that copper salts are less efficient in the  $\text{A}^3$  coupling reaction with primary amines, we chose cyclohexanecarboxaldehyde, aniline and phenylacetylene as model substrates to evaluate the title reaction in a molar ratio 1 : 1.1 : 1.2. Given that **1** consists of Cu(II), prolonged reactions were performed to allow reaction completeness and different solvents were used. To make the protocol more user-friendly, reactions were carried out in open air and room temperature. Reactions in various solvents (Table S1) afforded the anticipated product in good to moderate yields, and therefore DCM, a non-coordinating solvent, was chosen from this screening process.

Variation of catalyst loading determines the optimum condition when a 1.5% loading is applied (Table 1, Entries 1-5), while reactions in less time cause a significant drop in the

yield of **5aaa**. (Table 1, Entries 4,6,7) The reaction with copper salts provided similar yields; however, this was only achieved with higher catalyst loadings (10%), almost one order of magnitude more loading, which is in line with previous results (Table 1, Entry 8).<sup>[25]</sup> Given that the activation of alkynes is highly dependent on concentration,<sup>[31]</sup> the next step was to identify the limits of this catalytic system. Thus, we performed a reaction in higher concentration (1M) which yielded **5aaa** in moderate yields and identifying that the chosen 0.5M concentration is the optimum (Table 1, Entry 9).

**Table 1.** Optimisation of Reaction Conditions

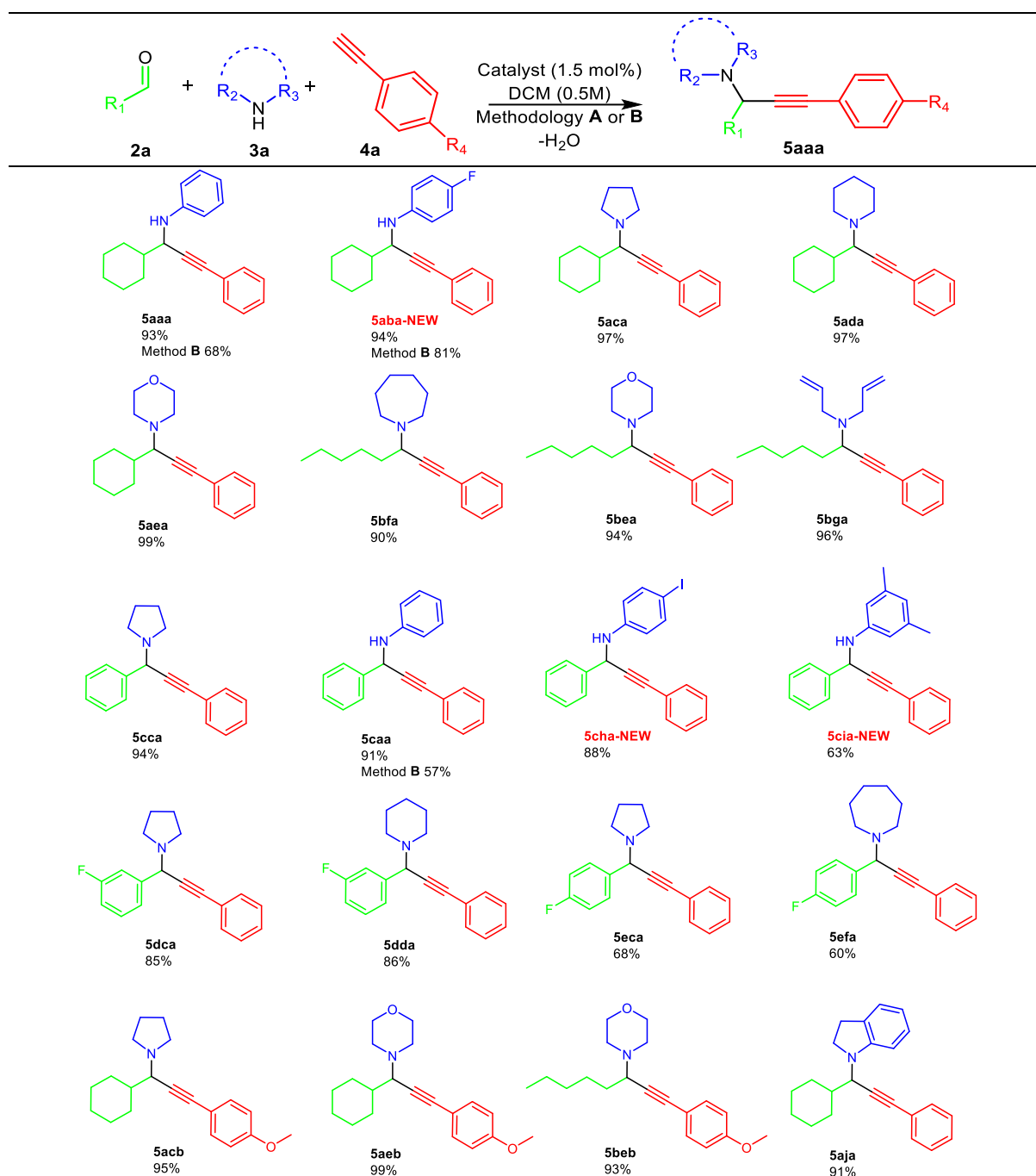


Entry	Loading (mol %)	Time (h)	Yield (%) <sup>a,b</sup>
1	5	24	53 <sup>c</sup>
2	3	24	74 <sup>c</sup>
3	2	24	95 <sup>c</sup>
4	1.5	24	93 <sup>c</sup>
5	1	24	53 <sup>c</sup>
6	1.5	12	52 <sup>c</sup>
7	1.5	6	30 <sup>c</sup>
8	10	24	99 <sup>d</sup>
9	1.5	24	81 <sup>e</sup>

<sup>a</sup>Relative yield calculated by <sup>1</sup>H-NMR based on the remaining **2a** and the intermediate Schiff base derived from **2a** and **3a**, <sup>b</sup>Reaction conditions: **1** (x mol%), 1.0 mmol aldehyde, 1.1 mmol amine, 1.2 mmol alkyne, molecular sieves 4Å, DCM and concentration 0.5 M based on aldehyde, <sup>c</sup>25°C and concentration 0.5 M.

<sup>d</sup>Reaction with 10 mol% Cu(OTf)<sub>2</sub>, <sup>e</sup>25°C and concentration 1 M,

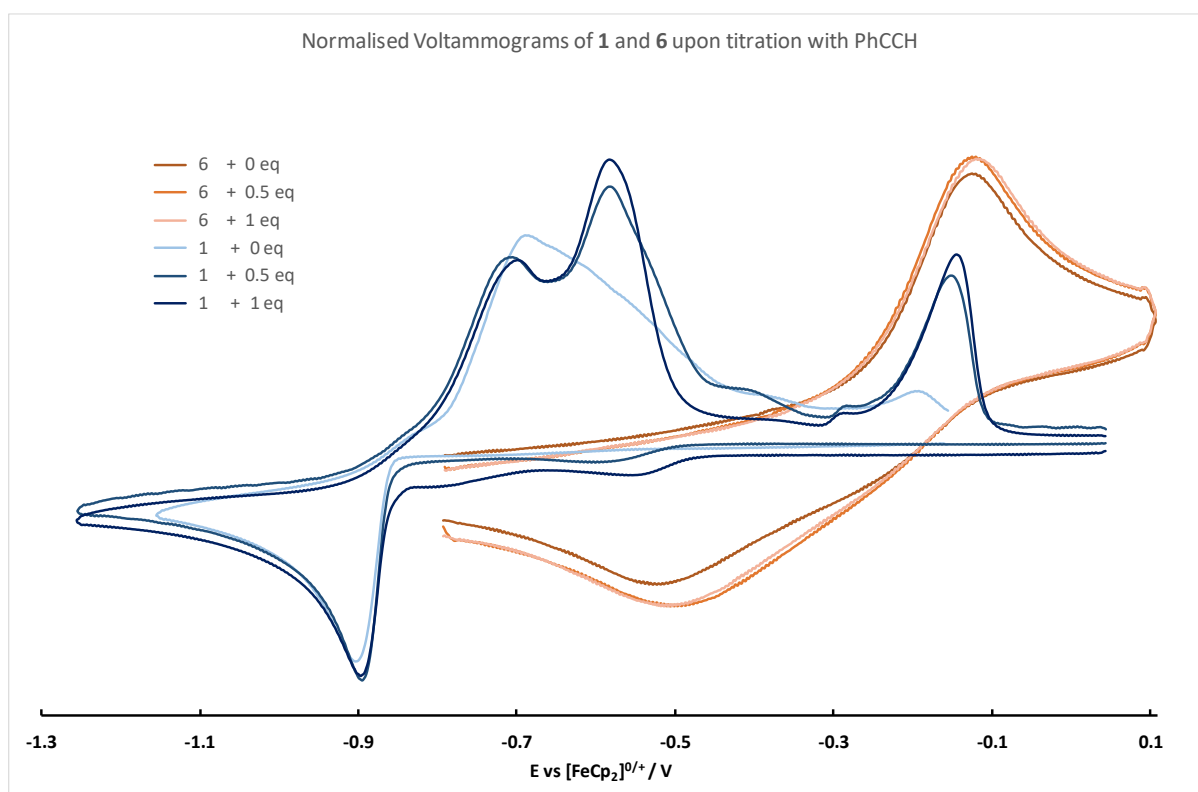
This methodology applies to a variety of primary and secondary, and its scope is extended affording twenty substrates, out of which three are synthesised and characterised for the first time (Table 2 and ESI for more details Fig S10-S39).

**Table 2.** Scope of the reaction with aldehydes, amines and alkynes.

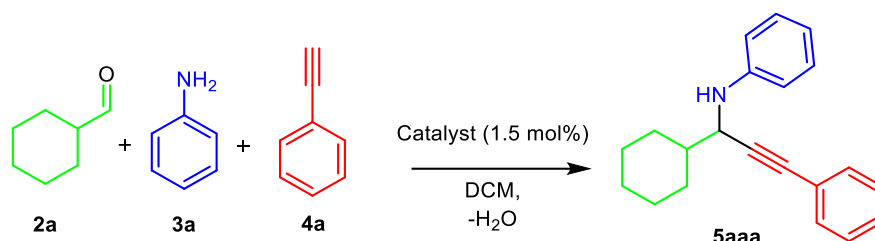
Isolated yields for the synthesis of propargylamines with 1.0 mmol aldehyde, 1.1 mmol amine, 1.2 mmol alkyne, molecular sieves, solvent DCM, concentration 0.5M based on aldehyde, promoted by **1** (1.5 mol%). Methodology **A**: stirring in open-air at 25°C for 24 hours. Methodology **B**: stirring under Ar at 25°C for 2 hours and relative yields were calculated by  $^1H$ -NMR based on the remaining **2a** and the intermediate Schiff base of **2a** and **3a**.

Aiming to shed light on the mechanism of the reaction and the applicability of the catalyst, the next step in our study was to perform reactions at elevated temperatures or microwave conditions as this has been noted in previous Cu(II) systems.<sup>[18–22]</sup> Indeed, under reflux (Table 3, entry 1) and microwave (Table 3, entry 2) conditions, the prototype reaction that affords **5aaa** is completed within one hour in excellent yields. Based on our recent studies,<sup>[26]</sup> we performed a series of reactions to gain mechanistic insights. A reaction for the

synthesis of **5cca**, in the presence of a radical trap (TEMPO, 10mol% based on aldehyde), afforded the expected product (Figure S40), thus excluding the formation of a radical species. The reactions at elevated temperature, under N<sub>2</sub> or Ar atmosphere, yielded product **5aaa** in a similar yield (Table 3, Entry 3), excluding the activation of the catalyst via bonding to dioxygen.<sup>[27]</sup> Finally, we performed a reaction under N<sub>2</sub> at room temperature for only two hours, and **5aaa** was obtained in a moderate yield (Table 3, Entry 4). The same reaction was repeated under Ar atmosphere (Table 3, Entry 5), providing the anticipated product in a similar yield. This unprecedented result provides us with a time-efficient synthetic protocol for the synthesis of propargylamines and will explore its potential in future. However, to shed light into this very exciting result, we performed cyclic voltammetry titrations, under N<sub>2</sub> atmosphere, of **1** in the presence of phenylacetylene (Figure 2 and S8). This study confirms a structural change into the catalytic system when one equivalent of phenylacetylene is added and could be explained based on ligand dissociation upon reduction of the copper centre and the formation of a {Cu(II/I)(pyb)<sub>x</sub>(Ph-C≡C-H)<sub>y</sub>} species.



**Figure 2** The cyclic voltammogram of **1** and **6** in the presence of phenylacetylene.

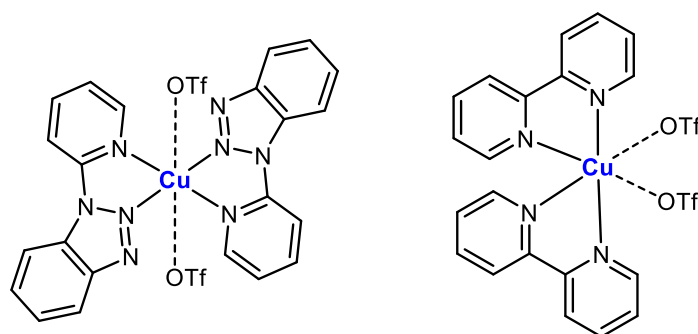
**Table 3.** Various experiments to obtain mechanistic evidence.

Entry	Time (h)	Atmosphere	Catalyst	Yield (%) <sup>a,b</sup>
1	1	Open air	<b>1</b>	95 <sup>c</sup>
2	1	Open air	<b>1</b>	96 <sup>d</sup>
3	2	N <sub>2</sub> /Ar	<b>1</b>	98 <sup>e</sup>
4	2	N <sub>2</sub>	<b>1</b>	65 <sup>f</sup>
5	2	Ar	<b>1</b>	68 <sup>f</sup>
6	2	Ar	<b>6</b>	Traces <sup>f</sup>
7	2	Ar	Cu(OTf) <sub>2</sub>	Traces <sup>g</sup>

<sup>a</sup>Relative yield calculated by <sup>1</sup>H-NMR based on the remaining **2a** and the intermediate Schiff base of **2a** and **3a**,

<sup>b</sup>Reaction conditions: **1** (1.5 mol%), 1.0 mmol cyclohexanecarboxaldehyde, 1.1 mmol aniline, 1.2 mmol phenylacetylene, molecular sieves 4Å, solvent DCM 2 mL, concentration 0.5 M, <sup>c</sup>80°C and concentration 0.5 M, <sup>d</sup>Microwave conditions 80°C and concentration 0.5 M. <sup>e</sup>80°C, <sup>f</sup>room temperature. <sup>g</sup> Loading 1 mol%

An attempt to rationalise how the A<sup>3</sup> coupling reaction is promoted from compound **1**, we decided to examine the catalytic efficacy of compound [Cu(bpy)<sub>2</sub>(OTf)<sub>2</sub>] (**6**)<sup>[9,28]</sup> (Figure S9). This compound has been structurally characterised and found to possess a *cis*-octahedral geometry (Scheme 2); thus, **1** and **6** have different stereochemistry. Notably, the catalytic reactions at room temperature under Ar atmosphere with **6** (2% loading, Table 3, entry 6) failed to provide the expected product. Besides, despite compound **6** shows a reversible CV signal,<sup>[9]</sup> a titration CV study with phenylacetylene identified a non-reversible signal (Figure S8) and the absence of precipitate or bpy moiety in the solution, in the crude <sup>1</sup>H-NMR. We may attribute this behaviour that complex **6** is stable, none of the bpy moieties diffuses to the solution during these titrations; thus a very stable {Cu(II)(bpy)<sub>x</sub>(Ph-C≡C-H)<sub>y</sub>} species is formed which prevents alkyne activation and the reaction to proceed. Given the short reaction time (1h), these results indicate that the stereochemistry of the pre-catalyst is vital for the formation of the active species, during the catalytic process, which is in line with literature evidence.<sup>[29,30]</sup> Given that even 1 mol% of the catalyst **1** still performs well while the other Cu(II) salts have been reported to perform poorly (Table 3, entry 7),<sup>[25]</sup> this discards a possible full ligand dissociation in **1** but favours the formation of a stable Cu(I)- complex which possibly is the active catalytic species. This suggestion can be further evidenced by the presence of pure ligand peaks in the crude NMR and LCMS data (Figures S41 and S42). Efforts to trap, monitor, isolate and characterise this Cu(I)-complex were unsuccessful. Besides, the absence of bulky groups in the pyridine or benzotriazole moieties, that would contribute steric effects and possibly prevent two different ligands from coordinating in the Cu(I) centre, prevented us from isolating and characterising this species in reactions with Cu(I) salts; this possibility will be explored in future studies.



**Scheme 2.** A chemical diagram of **1** and **6**, showcasing the *trans* and *cis* geometries.

To obtain further insight into the parameters governing the observed catalytic activity of **1**, calculations based on the Kohn-Sham Density Functional Theory (DFT) at the OLYP/TZP level of theory within the ZORA formalism was carried out, whereby meaningful, a comparison is made with **1**. In the absence of constraints due to environment, e.g. crystal packing effects, the optimised structure in the gas-phase possesses a non-planar geometry of the pyb ligands (Fig. 3), showcasing conformational lability through rotation around the central C-N bond, a feature not offered by bpy in **6**. Such flexibility should hence allow dispersion interactions with neighbouring atoms.

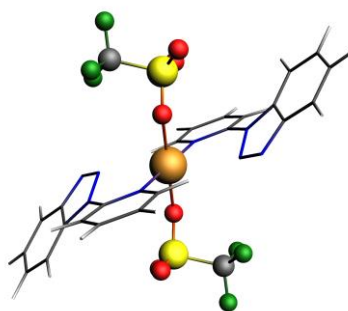


**Figure 3** Optimised gas-phase structure of **1**.

Inspection of molecular orbitals (MO) of **1** indicates a low-lying unoccupied beta (spin down) MO (Fig. 4). Upon removal of one OTf (**1a**), the degenerated levels split, but even in the lowered symmetry, the unoccupied level is conserved. Given the unhindered quasi-planar geometry (inset Fig. 4) and the alignment of in-phase  $p(N)-d(Cu)-p(N)$  orbitals as the main components spanning this unoccupied MO, binding to electron-rich molecules is thus facilitated. Furthermore, the presence of doubly degenerate levels points to potential symmetry lowering with concomitant lowering in energy hence possibly providing driving force towards reactivity. The slightly non-symmetrical deviation from planarity of the ligands upon the abstraction of OTf also points to another valuable property of the ligands. These neutral ligands can act as efficient charge sinks given the extended pi system and the ability to modulate conjugation through the C-N rotation thus accommodate charge density upon change of oxidation state or any reductive process. This can be depicted for instance by considering the molecular electrostatic potential on the calculated  $[Cu(I)L_2OTf]$  and  $[Cu(II)L_2OTf]$  (Fig 5) whereas the metal centres are relatively 'unchanged' the ligands get highly charged with high accumulation on the unbound nitrogen. This is in line with the frontier orbitals (see Fig. 3) showing that the unoccupied MOs are highly centred on the ligands. This speaks of the Cu centre just playing the role of a transit node in the system charge dynamics. Such property should facilitate the Cu(I)/Cu(II) redox equilibrium in the proposed



mechanism. One does see that the ligands allow simultaneous play and full synergic combination of electronic structure, geometrical dictum, vibronic contribution and charge flux dynamics.

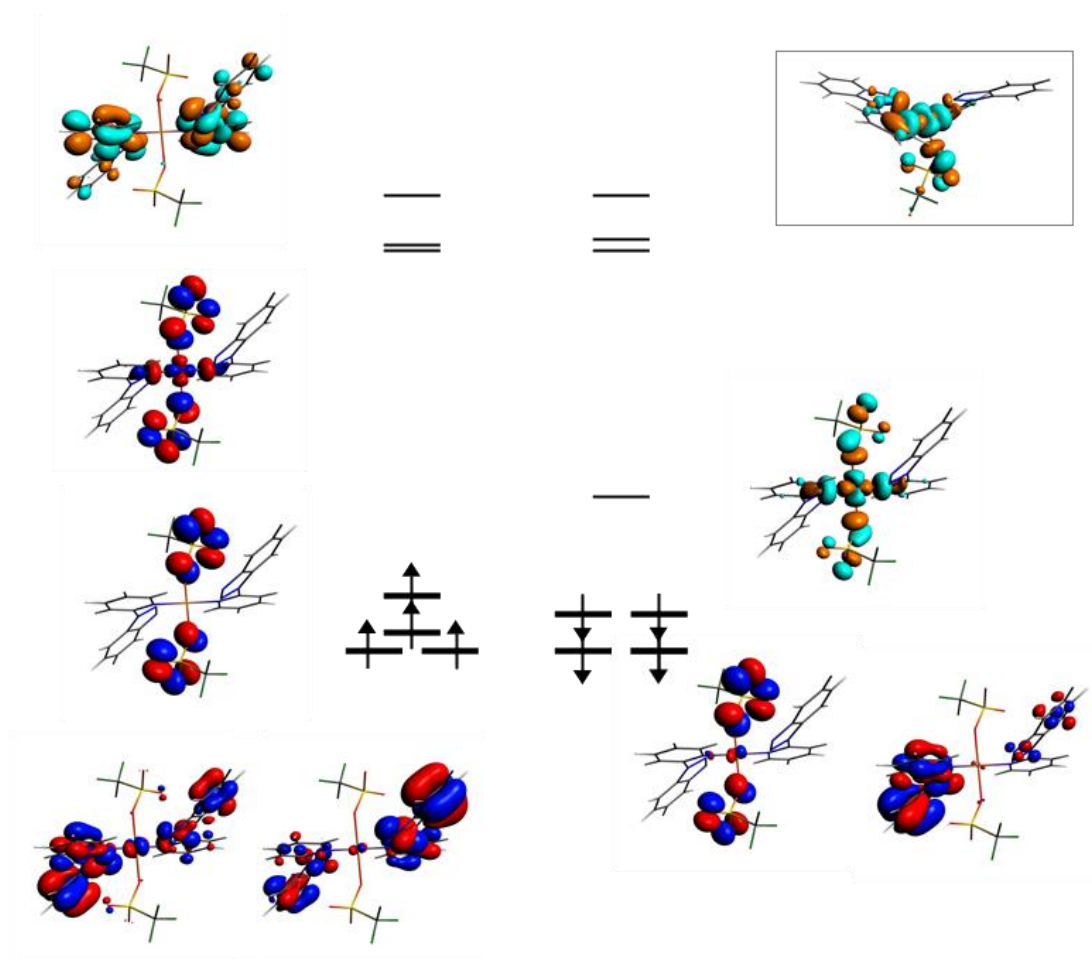


**Figure 4** Molecular orbital levels of **1**. Left: spin-up (alpha) electrons, Right: Spin-down (beta) electrons), levels in bold denote occupied levels, thin levels denote unoccupied levels. Inset: LUMO of compound **1a**.

The viability of key structures in the catalytic cycle were assessed with the aid of gas-phase calculations. Optimisation in the gas-phase reveals the flexibility of the ligands. Upon removal of one OTf ligand, rotation around C-N allows adopting a see-saw structure, possibly lowering the system energy. The Cu(I) analogue is highly energetic, probably exist as short-lived intermediate. In the intermediate geometries of  $[\text{Cu(I)}\text{L}_2(\text{OTf})(\text{HC}\equiv\text{CPh})]$ , and  $[\text{Cu(II)}\text{L}_2(\text{OTf})(\text{HC}\equiv\text{CPh})]$ , in the former the upon interaction of the alkyne with the metal, the triflate is displaced, leaving tetrahedral  $\text{Cu(I)}\text{L}_2$ , however, in the Cu(II) counterpart, the triflate is not displaced and the remaining  $\text{Cu(II)}\text{L}_2\text{OTf}$  adopts a see-saw geometry, identical to the structure previously described. In the case of the Cu(I), the departure of the OTf associated with increases in charge is aided by an additional stabilisation brought about by the two flanking ligands through dispersive interaction, this observation thus highly an equilibrium between the two oxidation states but with the  $[\text{Cu(I)}\text{L}_2(\text{OTf})(\text{HC}\equiv\text{CPh})]$  being favoured. Finally, alkyne capture and hydrogen abstraction proceed uniquely with Cu(I) which is not viable with Cu(II).

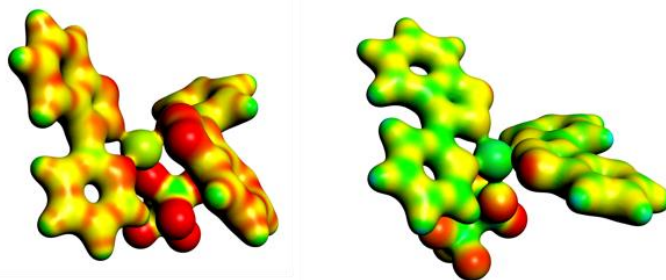
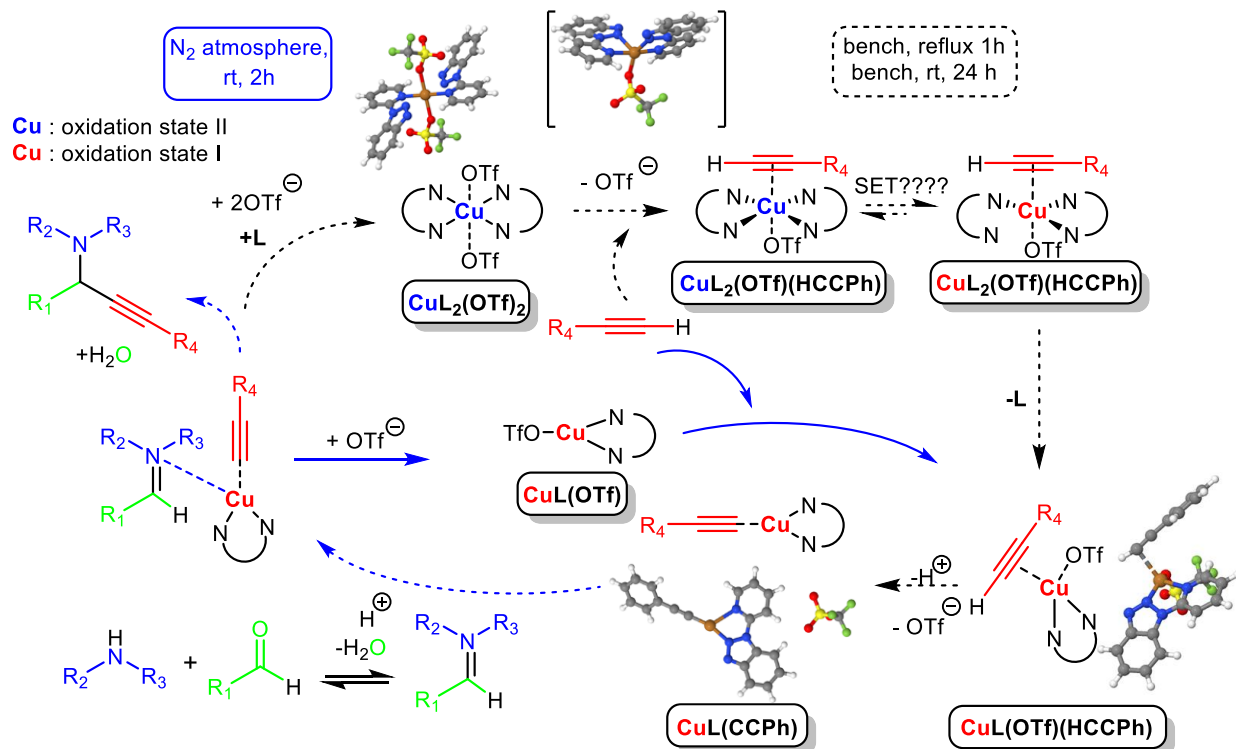


**Figure 5** The molecular electronic potential of [Cu(I)L<sub>2</sub>OTf] (left) and [Cu(II)L<sub>2</sub>OTf] (left)

Based on all these observations and bearing in mind that a) Cu should simultaneously binds both nucleophile (phenylacetylide) and electrophile (imine)<sup>[23]</sup> and b) the protocol proceeds in the absence of additional base or additives, we propose the catalytic mechanism shown in Scheme 2. This mechanism has two different paths. The external path (highlighted in dashed lines) involves the following steps: one OTf dissociation, alkyne binding, copper reduction through equilibrium of [Cu(II)L<sub>2</sub>(OTf)(HC≡CPh)] - [Cu(I)L<sub>2</sub>(OTf)(HC≡CPh)], ligand dissociation, OTf dissociation and acetylide activation, reaction with the imine and catalyst regeneration. The internal pathway (highlighted in blue) discards the reduction-oxidation process of the Cu centre but incorporates the triflate ion for the regeneration of the catalyst and alkyne activation purposes. Taking into account that the reduction of Cu(II) to Cu(I) by alkynes is a prolonged procedure,<sup>[31]</sup> we consider the formation of the Cu(I)-intermediate as the rate-determining step under ambient conditions, while under inert atmosphere the catalytic cycle can be achieved in almost 2 hours.



We report the first example of a Cu(II) complex *trans*-[Cu(II)(pyb)<sub>2</sub>(OTf)<sub>2</sub>] (**1**) that efficiently promotes the synthesis of propargylamines at room temperature through the A<sup>3</sup> coupling reaction. The labile character of the bridging N atom of the pyb is the key parameter, dictating ligand semi-flexibility and rotation and thus forming *in situ* the catalytic active {Cu(I)(pyb)(OTf)} species. By fine tuning the conditions, we significantly improve the time efficiency of this system from 24h to 2h. Experimental and theoretical comparison with the *cis*-[Cu(II)(byp)<sub>2</sub>(OTf)<sub>2</sub>] (**6**), suggest that stereochemistry of the pre-catalyst is vital for efficient C-H alkyne activation. The results presented herein pave the way for future discoveries and explorations in Coordination Chemistry, for bidentate ligands, and Catalysis, for reactions requiring substrate activation.

## Acknowledgements

## References

- [1] D. J. P. Kornfilt, D. W. C. Macmillan, *J. Am. Chem. Soc.* **2019**, *141*, 6853–6858.
- [2] S. Zhang, L. Zhao, *Nat. Commun.* **2019**, *10*, 4848.
- [3] M. A. Halcrow, *Chem. Soc. Rev.* **2013**, *42*, 1784–1795.
- [4] E. C. Constable, C. E. Housecroft, *Molecules* **2019**, *24*, 3951.
- [5] L. Gong, Z. Lin, K. Harms, E. Meggers, *Angew. Chemie - Int. Ed.* **2010**, *49*, 7955–7957.
- [6] K. K. Toh, Y.-F. Wang, E. P. J. Ng, S. Chiba, *J. Am. Chem. Soc.* **2011**, *133*, 13942–13945.
- [7] S. E. Allen, R. R. Walvoord, R. Padilla-Salinas, M. C. Kozlowski, *Chem. Rev.* **2013**, *113*, 6234–6458.
- [8] S. M. Barnett, K. I. Goldberg, J. M. Mayer, *Nat. Chem.* **2012**, *4*, 498–502.
- [9] P. Thongkam, S. Jindabot, S. Prabpai, P. Kongsaree, T. Wititsuwannakul, P. Surawatanawong, P. Sangtrirutnugul, *RSC Adv.* **2015**, *5*, 55847–55855.
- [10] C. Richardson, P. J. Steel, *Dalton Trans.* **2003**, *34*, 992–1000.
- [11] Z. Xu, D. S. Wang, X. Yu, Y. Yang, D. Wang, *Adv. Synth. Catal.* **2017**, *359*, 3332–3340.
- [12] R. Huang, Y. Yang, D. S. Wang, L. Zhang, D. Wang, *Org. Chem. Front.* **2018**, *5*, 203–209.
- [13] Q. Wu, L. Pan, G. Du, C. Zhang, D. Wang, *Org. Chem. Front.* **2018**, *5*, 2668–2675.
- [14] S. Pandey, T. Mandal, V. Singh, *ChemistrySelect* **2020**, *5*, 823–828.
- [15] V. A. Peshkov, O. P. Pereshivko, E. V. Van Der Eycken, *Chem. Soc. Rev.* **2012**, *41*, 3790–3807.
- [16] B. V. Rokade, J. Barker, P. J. Guiry, *Chem. Soc. Rev.* **2019**, *48*, 4766–4790.
- [17] V. A. Peshkov, O. P. Pereshivko, A. A. Nechaev, A. A. Peshkov, E. V. Van der Eycken, *Chem. Soc. Rev.* **2018**, *47*, 3861–3898.
- [18] C. J. Pierce, C. H. Larsen, *Green Chem.* **2012**, *14*, 2672–2676.
- [19] C. E. Meyet, C. J. Pierce, C. H. Larsen, *Org. Lett.* **2012**, *14*, 964–967.
- [20] B. Agrahari, S. Layek, R. Ganguly, D. D. Pathak, *New J. Chem.* **2018**, *42*, 13754–13762.
- [21] K. Lauder, A. Toscani, N. Scalacci, D. Castagnolo, *Chem. Rev.* **2017**, *117*, 14091–14200.
- [22] E. Loukopoulos, M. Kallitsakis, N. Tsoureas, A. Abdul-Sada, N. F. Chilton, I. N. Lykakis, G. E. Kostakis, *Inorg. Chem.* **2017**, *56*, 4898–4910.
- [23] C. Koradin, K. Polborn, P. Knochel, *Angew. Chemie - Int. Ed.* **2002**, *41*, 2535–2538.
- [24] G. Zhang, H. Yi, G. Zhang, Y. Deng, R. Bai, H. Zhang, J. T. Miller, A. J. Kropf, E. E. Bunel, A. Lei, *J. Am. Chem. Soc.* **2014**, *136*, 924–926.
- [25] C. E. Meyet, C. J. Pierce, C. H. Larsen, *Org. Lett.* **2012**, *14*, 964–967.

- [26] S. I. Sampani, V. Zdorichenko, M. Danopoulou, M. C. Leech, K. Lam, A. Abdul-Sada, B. Cox, G. J. Tizzard, S. J. Coles, A. Tshipis, et al., *Dalton Trans.* **2020**, 49, 289–299.
- [27] D. S. Peters, F. E. Romesberg, P. S. Baran, *J. Am. Chem. Soc.* **2018**, 140, 2072–2075.
- [28] T. Stopka, L. Marzo, M. Zurro, S. Janich, E.-U. Würthwein, C. G. Daniliuc, J. Alemán, O. G. Mancheño, *Angew. Chemie Int. Ed.* **2015**, 54, 5049–5053.
- [29] J. A. Schachner, B. Terfassa, L. M. Peschel, N. Zwettler, F. Belaj, P. Cias, G. Gescheidt, N. C. Mösch-Zanetti, *Inorg. Chem.* **2014**, 53, 12918–12928.
- [30] J. A. Schachner, B. Berner, F. Belaj, N. C. Mösch-Zanetti, *Dalton Trans.* **2019**, 48, 8106–8115.
- [31] S. N. Semenov, L. Belding, B. J. Cafferty, M. P. S. Mousavi, A. M. Finogenova, R. S. Cruz, E. V. Skorb, G. M. Whitesides, *J. Am. Chem. Soc.* **2018**, 140, 10221–10232.